Proceedings World Geothermal Congress 2026
Calgary, Canada, June 8 – 11, 2026

An Integrated 3D Workflow for Hot Sedimentary Aquifer Characterization to Support Enhanced Geothermal System Development

Emilie Gentry[1]*and Kiley Baird[1]
Teverra LLC[1]*
*kiley.baird@teverra.com

Keywords: Hot Sedimentary Aquifer, 3D Modeling, Enhanced Geothermal Systems

ABSTRACT

Hot sedimentary aquifers (HSAs) in sedimentary basins represent an important target for Enhanced Geothermal Systems (EGS). Their successful development requires consistent integration of geological, thermal, petrophysical, and geomechanical information across scales, from regional screening to field-scale design. This paper describes an integrated three-dimensional workflow that couples basin-scale thermal modeling, 3D geological modeling, reservoir property characterization, dynamic thermohydraulic simulation, and geomechanical and thermo–hydro–mechanical (THM) analysis. The workflow is designed to be portable between basins, to maintain internal consistency between the different technical domains, and to explicitly propagate uncertainty through the modeling chain. Rather than document a specific site, we present the methodology, data handling, and modeling decisions in sufficient detail that the workflow can be replicated and adapted to other HSA–EGS settings.

1 INTRODUCTION

The utilization of hot sedimentary aquifers for EGS development is often limited more by uncertainty than by absolute resource potential (Baird, 2025; Birdsell et al., 2024; Limberger et al., 2018; Moeck, 2014). Temperature at depth, thickness and connectivity of the target unit, and the in-situ stress state all exert strong control on feasible flow rates and sustainable power output. In sedimentary geothermal systems, large-scale geological architecture and connectivity often exert greater control on reservoir performance than small-scale variations in petrophysical properties, as fluid-flow pathways ultimately govern heat transport and production sustainability (Baird, 2025; Ringrose and Bentley, 2021). Traditional approaches (Khalili and Ahmadi, 2024) tend to address these questions in sequence and in isolation: Geological modeling occurs at the basin-scale, followed by reservoir modeling, then numerical simulations. This separation produces singular deterministic models that are heavily data-driven rather than rooted in geoscientific understanding (Ringrose and Bentley, 2021).

The workflow described here was developed to avoid that fragmentation. It is explicitly three-dimensional and fully integrated across domains. We begin with available drilling, geological, and thermal data; construct a basin-scale thermal and geological model; derive reservoir properties and scale them appropriately; perform dynamic thermohydraulic simulations; and then use the resulting pressure and temperature fields as inputs to geomechanical and THM analysis. The process is not strictly linear; feedback loops allow updates to propagate in both directions. For example, geomechanical constraints can inform plausible permeability distributions, and reservoir simulation results can highlight data needs for further characterization.

Geological modelling was carried out in Leapfrog Energy (Seequent) to construct the three-dimensional stratigraphic and structural framework and to populate petrophysical and thermal properties. Reservoir simulations were performed in Volsung (Seequent), which was used to model coupled fluid flow and heat transport and to evaluate long-term thermal production under different development scenarios.

The three-dimensional geomechanical model was implemented using the VISAGE finite-element geomechanics simulator through its integration with the structural and property models (SLB). The geomechanical grid and mechanical properties were constructed from the geological model, and boundary stresses were applied and calibrated to match one-dimensional stress profiles at well locations. Pressure and temperature changes from the Volsung reservoir simulations were then applied to the geomechanical model to evaluate coupled thermo–hydro–mechanical behavior, including stress changes, deformation, and fault reactivation potential.

For clarity, the paper is organized by workflow stage. However, in application these stages overlap and iterate. At several points we indicate where figures and tables would typically be introduced in a conference paper to illustrate intermediate results and key decisions.

2 DATA AND PREPROCESSING

2.1 Regional Context and Objectives

The starting point for the workflow is a clear definition of the regional and operational objectives. At the basin scale the aim is usually to map the depth and temperature of candidate HSA units, identify areas where the combination of temperature, thickness, and permeability is favorable, and eliminate areas where conditions are clearly suboptimal. At the field scale the objective shifts to testing specific development concepts, such as doublets or small well clusters, and to assessing drilling risk and induced seismicity potential. In both cases, the key requirement is a consistent data foundation.

2.2 Thermal Data and Bottom-Hole Temperature Corrections

Thermal data are derived primarily from bottom-hole temperatures (BHTs) and wireline logs where available (Figure 1). Because BHTs are affected by drilling disturbance, corrections are applied using Horner-type approaches, with correction strategy varying according to data quality and metadata availability (Horner, 1951). Quality control includes cross-plots of temperature versus depth, comparison with neighboring wells, and identification of anomalous values associated with convective disturbance or shallow aquifers. Corrected temperatures are used to construct a conductive thermal model based on cumulative thermal resistance (Bullard, 1939; Carslaw & Jaeger, 1959).

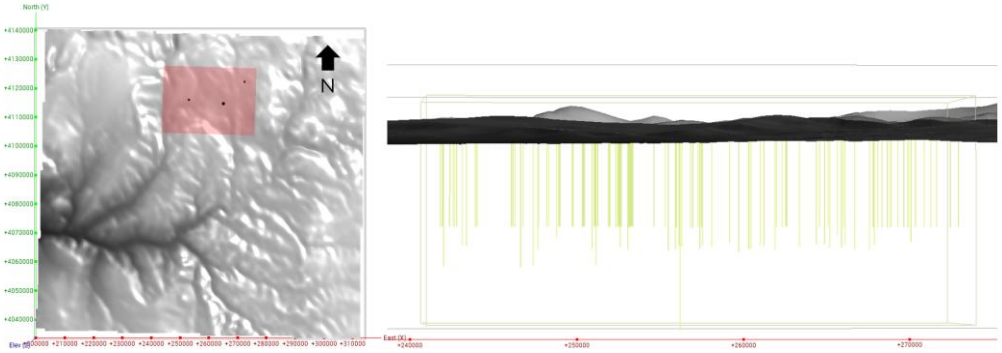


Figure 1. Map and 3D geologic model showing selcted wells that BHT corrections are appied to.

2.3 Stratigraphic and Structural Data

The geological basis of the model consists of formation tops interpreted from well logs, regional stratigraphic charts, and surface geological mapping. These data are reconciled into a single stratigraphic framework that defines the vertical ordering of units, their typical thickness ranges, and key unconformities. Where different naming conventions exist between fields or operators, a harmonization step is performed so that each 3D horizon corresponds to a clearly defined stratigraphic concept.

Structural information is taken from regional tectonic maps, published cross sections, and any available seismic interpretation. Even where deformation is relatively mild, the presence of gentle warping, small-offset faults, or long-wavelength tilting is important to capture, since these features can alter both reservoir geometry and stress orientation. Only structures that can be supported by multiple lines of evidence are carried forward into the 3D model; speculative features are avoided unless their presence is required to reconcile contradictory well data.

The stress regime and rheological properties used in the geomechanical models are derived from a combination of well log data, well test data, and regional stress information. Vertical stress is calculated from integrated density logs, while pore pressure is estimated from hydrostatic gradients and calibrated where possible using well test data. Minimum horizontal stress is constrained using leak-off tests and diagnostic fracture injection tests, and maximum horizontal stress orientation is inferred from borehole image logs, drilling-induced fractures, and regional stress compilations. Rock mechanical properties, including Young's modulus, Poisson's ratio, unconfined compressive strength, and friction angle, are estimated from sonic and density logs using established empirical correlations and calibrated where possible with laboratory measurements. Mechanical stratigraphy is defined at the formation scale to represent rheological layering within the sedimentary sequence, which is critical for predicting stress distribution, fracture containment, and fault reactivation potential (Zoback, 2010; Barton et al., 1995; Zang and Stephansson, 2010).

2.4 Rock and Fluid Properties

Rock thermal properties are assigned at the formation level. For each stratigraphic unit we define a plausible range of thermal conductivity, volumetric heat capacity, and radiogenic heat production. These values are obtained from a combination of local measurements, if available, and analog formations in similar basins. Fluid properties (density, viscosity, compressibility, and specific heat) are represented as functions of temperature and pressure, consistent with the brine composition expected for the HSA setting.

In sedimentary basins, fluid salinity and composition can vary significantly between formations and laterally across the basin due to depositional environment, diagenesis, and fluid migration. Where direct fluid samples are not available, salinity ranges are estimated from regional hydrogeological studies, formation water databases, or analog basins, and fluid properties are adjusted accordingly as functions of temperature, pressure, and salinity.

Petrophysical properties such as porosity and permeability are derived from well logs, core analysis, and analog studies. For the target HSA, it is common to find only a handful of wells with modern logging suites or core coverage; we therefore develop porosity–permeability transforms, such as variants of the Kozeny–Carman relationship (Dvorkin, 2009), and supplement these with data from outcrop or nearby producing fields where sedimentological and diagenetic conditions are comparable.

3 THREE-DIMENSIONAL GEOLOGICAL AND THERMAL MODELING

3.1 Model Domain and Discretization

The 3D geological model covers the portion of the basin where the HSA is both present and of potential interest (Figure 2). Lateral extents are usually selected so that the HSA unit and its bounding formations are fully captured, and so that model boundaries do not intersect the region of high interest too closely. Vertically, the model spans from the near-surface, where boundary conditions are imposed, down to crystalline basement or to a depth beyond the base of the HSA.

The model is discretized into a geocellular grid. In the early stages, cell sizes can be on the order of hundreds of meters laterally and tens of meters vertically. This resolution is sufficient to represent regional thickness trends and to host the thermal solution while remaining computationally efficient. Later, as the focus narrows to a particular development area, higher resolution sub-volumes are extracted.

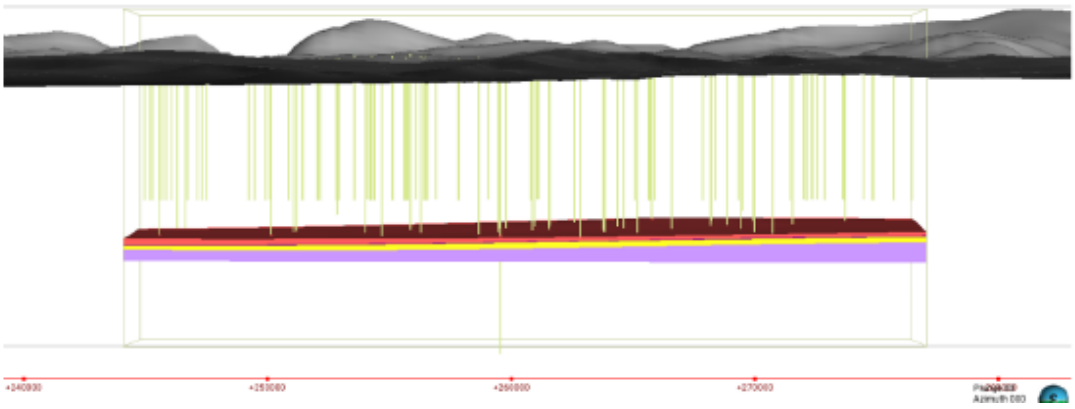


Figure 2. 3D view of the stratigraphic surfaces and the gridded representation, with the HSA highlighted in yellow.

3.2 Stratigraphic Interpolation and Structural Framework

Formation tops from wells are interpolated using algorithms such as minimum curvature or kriging, constrained to honor structural trends and known faults. Where seismic surfaces are available, they are used as primary guides for deeper horizons, with well control used for local calibration. Faults are introduced as explicit discontinuities, represented either as surfaces or as transmissibility multipliers at the grid scale.

A key decision concerns the level of stratigraphic detail to be retained. The workflow distinguishes between units that materially affect the hydraulic and thermal behavior (for example, the HSA itself and strong seals above and below) and units that primarily contribute thermodynamic variability (Wang et al., 2023). The former are modeled with greater vertical detail; the latter may be grouped into thicker composite layers to keep the model tractable.

3.3 Basin-Scale Conductive Thermal Model

Thermal conductivity controls the rate of heat transfer in the subsurface and is a key parameter in geothermal modeling. It is influenced by mineralogy, porosity, fluid saturation, and effective stress, resulting in variability both within and between formations, often by a factor of 2–3 for similar lithologies. In numerical models, thermal conductivity is typically upscaled to the formation scale (Rühaak et al., 2015).

Direct measurement of thermal conductivity was not feasible in this study, as temperature data were derived from BHTs rather than core-scale measurements. Instead, a representative stratigraphic column constructed from well logs and regional basin data was used to assign thermal conductivity values by lithology based on published literature. Modeled temperatures are calibrated against corrected BHTs following established regional geothermal methodologies (Blackwell & Richards, 2004).

3.4 Uncertainty and Scenario Construction

Thermal model uncertainty is quantified by generating multiple realizations that sample plausible ranges of thermal conductivity, heat production, and basal heat flow. For each realization, temperature at depth is recalculated, and the ensemble of outcomes defines a probabilistic temperature distribution at any given location. These distributions are then carried forward into the reservoir modeling stage as alternative initial conditions.

The number of realizations is chosen to balance computational cost and coverage of the parameter space. In many cases a small set of representative scenarios, for example low, base, and high temperature cases, is sufficient to bracket the range of interest for early decision-making.

4 RESERVOIR PROPERTY MODELING AND UPSCALING

4.1 Porosity and Permeability in the HSA

Within the HSA unit, porosity is modeled as a function of depth, facies, and local well log availibility within the basin. Empirical compaction trends often provide the first-order control, with deviations assigned where evidence for anomalous diagenesis exists. Permeability is then derived from porosity through established transforms, with different parameter sets applied to distinct facies where justified (Table 1).

Because direct permeability measurements are typically sparse, the workflow treats permeability as a key uncertain parameter. Multiple conceptual models are considered, including spatially homogeneous permeability, gradual lateral trends (for example, proximal–distal transitions), and zoned models reflecting channel–overbank architectures or shoreface–offshore transitions. Each conceptual model results in a distinct 3D permeability field. However, dual fracture-matrix permeability is upscaled in this study to increase computational efficiency.

Porosity–permeability transforms follow compaction and diagenetic trends widely described in reservoir engineering literature (Grant et al., 2011). Upscaling techniques follow Haldorsen & Lake (1984) and the field-focused guidance of Ringrose & Bentley (2021).

Conceptual permeability models and heterogeneity representations follow practices described in Caers (2011) and Journel & Huijbregts (1978).

Table 1. Petrophysical parameters assigned to each geological unit. For the purpose of this study, we assume density, specific heat, and thermal conductivity to be the same as to focus on other independent variables.

Unit	Overburden (Unknown)	Sandstone 1	Sandstone 2	Sandstone 3	Sandstone 4	Underburden (Unknown)
Porosity (%)	5	10	0.01	10	0.01	0.01
Permeability (mD)	1	950	0.01	variable	0.01	0.01
Density (kg/m3)	2600					

Specific Heat (kJ/(kg*K)	1
Thermal Conductivity (W/(m*K)	5.5

4.2 Heterogeneity and Connectivity

The representation of heterogeneity depends on the scale and purpose of the model. At basin scale, heterogeneity is expressed primarily as broad trends in thickness and average properties. At field scale, the model may include finer-scale features, such as subtle intraformational barriers or higher-permeability layers. Where detailed facies models are not available, stochastic methods are used to generate plausible spatial patterns that honor the available data and geological understanding (Wang et al., 2021).

Connectivity is evaluated through flow-based metrics, such as the distribution of transmissivity between potential well locations. These analyses help identify whether reservoir performance will be dominated by a few preferential pathways or by more distributed flow, and they inform the choice of well spacing and pattern.

4.3 Upscaling for Dynamic Simulation

The geologic model may often be of too high resolution to complete a full-scale numerical simulation in a reasonable timeframe and cost, especially when long time horizons and multi-parameter uncertainty analyses are required. Upscaling is therefore applied, aggregating fine cells into coarser blocks while preserving key flow and storage properties (Figure 3). While true reservoir properties may involve dissolved or entrapped gasses, here we upscale the reservoir fluid to be single-phase pure water

Upscaling is performed separately for each conceptual permeability model, yielding a family of reservoir grids that are structurally identical but differ in effective permeability distributions. Where strong anisotropy exists, directional upscaling is applied so that the coarser grid preserves the directional transmissivity behavior of the fine-scale model. Permeability anisotropy in sedimentary geothermal reservoirs may arise from depositional setting (e.g., bedding and cross-bedding), stratigraphic layering, fracture networks, stress-aligned microfractures, and fault-related permeability anisotropy (Ringrose and Bentley, 2021). These anisotropic trends are evaluated using a combination of well logs, core measurements, outcrop analogues, image logs, well test interpretation, and regional structural analysis**.** Directional transmissibility is then preserved during upscaling so that the dynamic simulation reflects the dominant flow directions present in the geological model.

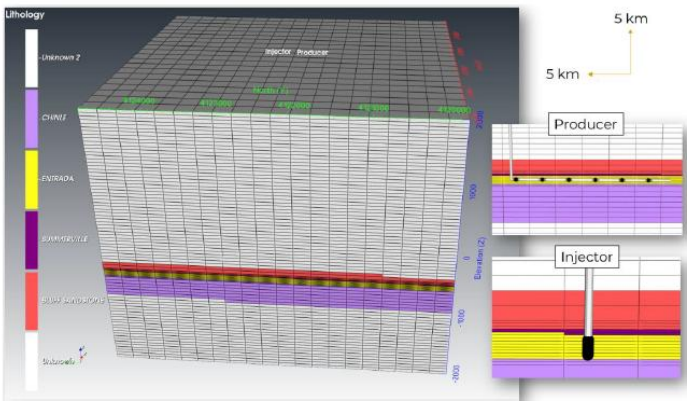


Figure 3. Final reservoir model of the AOI from surface to 4 km depth. Cross-sections of the wells within the refined grid cells are shown on the right.

5 DYNAMIC THERMOHYDRAULIC SIMULATION

5.1 Initial and Boundary Conditions

Initial pressure conditions are defined by hydrostatic or slightly overpressured gradients, consistent with regional observations. Initial temperature is taken from the basin-scale thermal model, ensuring that the reservoir simulation starts from a thermally consistent state. At the outer boundaries of the model, no-flow

conditions are imposed for mass, while temperature is either fixed at far-field values or treated with a constant heat-flux condition. Vertically, the over- and underlying units provide thermal and hydraulic confinement as determined by their assigned properties.

5.2 Operational Scenarios and Performance Metrics

The workflow evaluates a range of operational scenarios, including variations in well spacing, number of production–injection pairs, injection temperature, and control strategy. Some scenarios emphasize constant-rate production to examine thermal drawdown, while others use pressure-limited operation to assess achievable flow rates under stress or regulatory constraints.

Performance is quantified using metrics such as cumulative produced energy, production temperature decline, net electrical power, and time to reach defined thermal or pressure limits. Net electrical power is calculated by applying mass rates based on a standardized curve of wellhead pressures, and the resulting net power output is evaluated across a range of reservoir and operational parameters (Figure 4). Simulations are typically run over multi-decade time periods to capture long-term thermal and hydraulic behavior.

Figure 4 shows the sensitivity of electrical power output after 30 years of production to key reservoir and operational parameters. Of the parameters evaluated, basal temperature has the strongest influence on long-term power generation, with higher temperatures producing significantly greater power output due to the direct relationship between produced fluid enthalpy and power generation. Permeability also has a strong impact, particularly in the lower permeability range, where increases in permeability result in substantial gains in flow rate and therefore power output. However, at higher permeability values the benefit begins to plateau, indicating that other factors such as thermal breakthrough and well spacing begin to control performance.

Well spacing influences long-term performance by controlling thermal sweep efficiency and the timing of thermal breakthrough. Larger well spacing generally results in higher power output at 30 years due to delayed thermal breakthrough and improved heat extraction from a larger reservoir volume. Production strategy also affects performance, with fixed mass flow rate generally producing higher power output but also showing greater variability, while fixed wellhead pressure provides more stable but slightly lower power output. Overall, the results indicate that reservoir temperature and permeability are the primary controls on power generation, while well spacing and operational strategy act as secondary controls that influence the sustainability and stability of production over time.

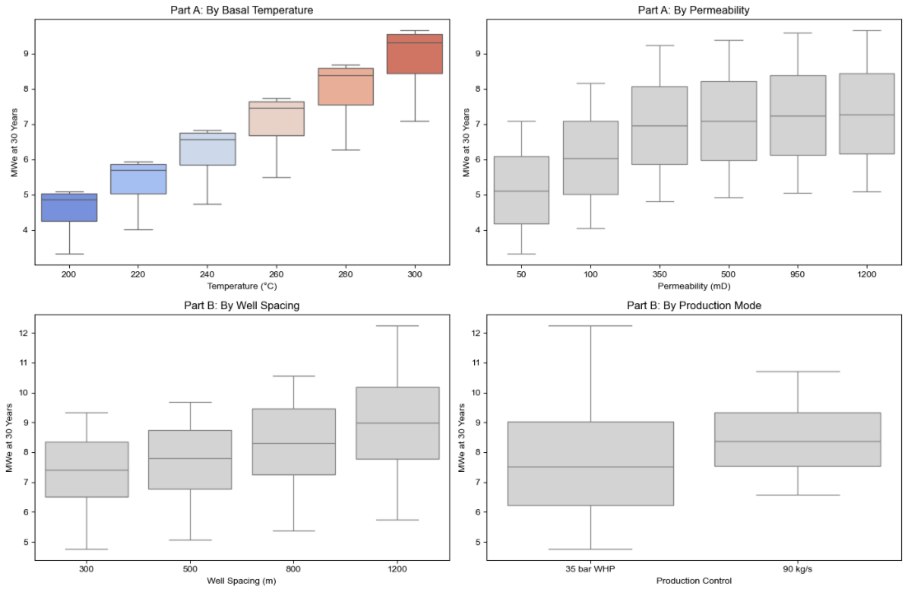


Figure 4. Sensitivity of MWe power output at 30 years to key parameters.

5.3 Sensitivity and Uncertainty Analysis

Sensitivity analysis is performed by varying key uncertain parameters, including permeability distribution, reservoir temperature, and operational controls, and evaluating their impact on performance metrics. Figure 5 summarizes the relative sensitivity and uncertainty associated with key parameters controlling geothermal reservoir performance. Permeability and thermal breakthrough are identified as the most influential parameters, indicating that reservoir connectivity and flow pathways exert the strongest control on long-term energy

production and system sustainability. Temperature also shows a high influence, reflecting its direct control on produced fluid enthalpy and therefore power generation. Well spacing has a moderate influence, as it primarily affects the timing of thermal breakthrough rather than initial production rates. Pump performance and surface constraints show comparatively lower influence on long-term reservoir performance, although they remain important for operational feasibility and economic performance.

The chart also highlights that the parameters with the greatest impact on performance are often those with the highest uncertainty, particularly permeability distribution and reservoir connectivity. This reinforces the need for integrated geological, reservoir, and geomechanical modeling to reduce uncertainty in these parameters and to evaluate development scenarios across a range of plausible reservoir conditions.

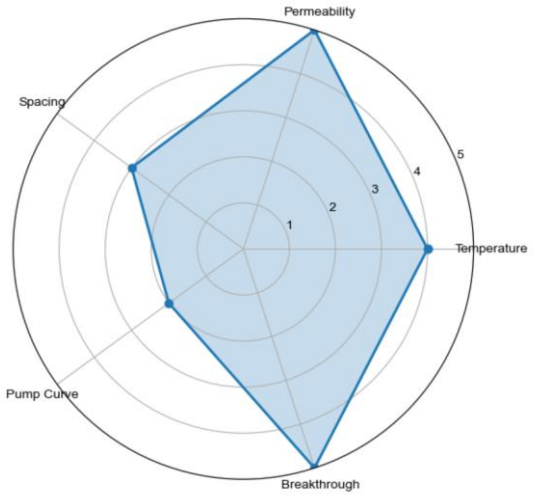


Figure 5. Uncertainty and sensitivity radar chart. This chart summarizes the relative impact and uncertainty of key geothermal reservoir modeling parameters. Each axis represents a parameter scored from 0 (low impact) to 5 (high impact).

6 GEOMECHANICAL AND THM WORKFLOW

6.1 One-Dimensional Geomechanical Models

Before constructing a full 3D geomechanical model, one-dimensional models are built at key well locations. These models derive vertical stress from integrated density logs, estimate pore pressure from hydrostatic assumptions or empirical relationships, and constrain minimum and maximum horizontal stresses using leak-off tests, image log interpretations, and regional stress compilations. Vertical and horizontal stresses are calculated following the principles of Zoback (2010), with rock strength relationships informed by empirical UCS/elastic modulus correlations. DFIT- and LOT-based stress constraints follow methods established in Zang & Stephansson (2010).

From these data, we construct a depth-dependent stress profile and evaluate the wellbore stability of both existing and planned well trajectories. The safe operational window, typically expressed in terms of equivalent mud weights for drilling and acceptable drawdown or injection pressures for production, is quantified (Figure 6). These one-dimensional models also provide important calibration targets for the subsequent 3D geomechanical model.

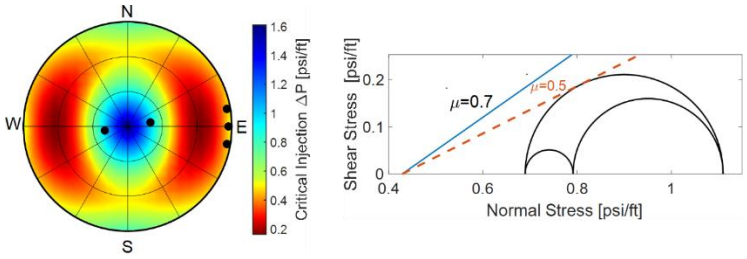


Figure 6. (Left) Stereonet showing the critical injection pressure difference (ΔP) required for slip on pre-existing fractures. Fractures in formation of interest are indicated by points on the stereonet. (Right) Mohr diagram comparing failure envelopes for friction coefficients μ = 0.7 and μ = 0.5.

6.2 Three-Dimensional Geomechanical Model Construction

The 3D geomechanical model uses the same structural framework as the geological and reservoir models to ensure consistency (Figure 7). Rock mechanical properties are populated using the petrophysical model, and boundary conditions are set such that the modeled stress field reproduces the 1D constraints at well locations. The model domain is usually larger than the reservoir model to minimize boundary effects on the stress field in the area of interest.

Within the HSA and its immediate surroundings, the mesh is refined to capture local stress perturbations arising from heterogeneity or operational loading. The initial model is calibrated by adjusting boundary stresses and, where necessary, mechanical property distributions until the predicted stress state at calibration wells aligns with the 1D models within acceptable tolerances. Mechanical property distribution and boundary condition specifications follow the methodological framework provided by Zoback (2010). Stress calibration uses principles described in Barton, Zoback & Moos (1995) regarding critically stressed fractures.

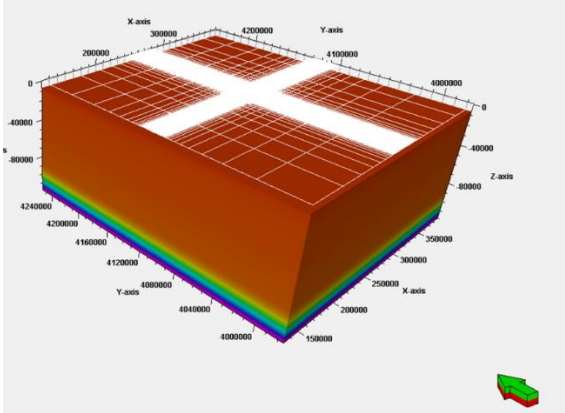


Figure 7. Embedded grid structure of the 3D geomechanical model. A high-resolution grid is applied to the reservoir zone, nested within a coarser full-domain mesh.

6.3 Fracture Network and Slip Tendency

Discrete fracture networks are introduced to represent the likely distribution of natural fractures that could become hydraulically or mechanically active. Orientation sets are informed by regional structural trends and, where available, image log interpretations or outcrop measurements. Fracture densities and apertures are assigned based on conceptual models consistent with the lithology and tectonic setting.

The slip tendency of fractures is evaluated under the modeled stress field by comparing resolved shear and normal stresses on fracture planes to frictional strength. This analysis identifies fractures that are close to failure under current conditions and therefore most sensitive to changes in pore pressure or temperature. The results define critical orientations and depths where injection may be more likely to induce slip.

6.4 Thermo–Hydro–Mechanical Coupling and Induced Seismicity

To evaluate induced seismicity risk, the geomechanical model is coupled to reservoir pressure and temperature changes derived from dynamic simulations (Figure 8). In this coupling, time-dependent pore pressure and temperature fields are applied to the geomechanical grid, and incremental stresses are computed. Thermal contraction or expansion and pore pressure changes both contribute to modifications of effective stress. Permeability–stress coupling, thermal stress changes, and fault slip processes follow the THM formulations discussed in Rutqvist (2015). Induced seismicity analysis references global frameworks reviewed by Majer et al. (2007) and pressure-mediated triggering described by Ellsworth (2013).

Two operational archetypes are typically compared. In the unbalanced case, injection volumes are not matched by production, and pressure tends to accumulate in the formation. In the balanced case, injected and produced volumes are closely matched, and net pressure buildup is minimized. The THM simulations show that, in general, balanced operation leads to smaller and more localized stress perturbations and therefore a lower potential for fault reactivation.

The modeling outputs include the temporal evolution of stress, the distribution of Coulomb failure changes on fractures, and indicative magnitudes of possible seismic events based on slip area and stress drop

assumptions. These results inform the design of monitoring networks, traffic-light protocols, and operational limits on injection pressures or rates.

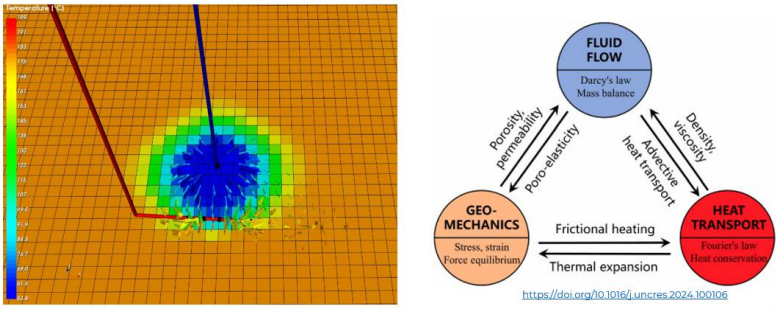


Figure 8. Schematic showing the relationship of geomechanical modeling, heat transport, and fluid flow and how these are important for the wellbore modeling in a HSA.

7 INTEGRATION AND ITERATION

A central feature of the workflow is that no model is considered final. As new information becomes available, whether from additional drilling, logging, well testing, or monitoring, it is incorporated and used to update the relevant model components. For example, measured injectivity from a test well may narrow the plausible range of permeability and hence reduce uncertainty in the reservoir simulations. Similarly, improved knowledge of stress orientation from image logs can refine both the geomechanical model and the expected performance of fracture-dominated flow paths.

Information moves in both directions. Geomechanical constraints can indicate that certain high-permeability scenarios are unlikely because they would require unrealistically low effective stresses, while reservoir simulations can show that some conceptual permeability models fail to reproduce observed pressure responses. The integrated framework allows these contradictions to be identified and resolved rather than ignored. Feedback between reservoir simulation and geomechanics follows the iterative multi-domain framework advocated by Ringrose & Bentley (2015). Uncertainty reduction is targeted using methods described in Finsterle (2015) and Caers (2011).

8 CONCLUSIONS

This paper has presented an integrated three-dimensional workflow for the characterization and development assessment of hot sedimentary aquifers in the context of Enhanced Geothermal Systems. The workflow integrates basin-scale thermal modeling, three-dimensional geological modeling, reservoir property characterization, dynamic thermohydraulic simulation, and geomechanical and thermo–hydro–mechanical analysis within a consistent structural and property framework. By linking these domains, pressure, temperature, and stress changes can be evaluated in a physically consistent manner across the full system.

The results demonstrate that long-term geothermal performance in sedimentary systems is controlled primarily by reservoir temperature, permeability distribution, and reservoir connectivity, while operational parameters such as well spacing and production strategy influence the sustainability and stability of production. At the same time, geomechanical constraints define the operational pressure limits within which these systems must operate. An integrated workflow is therefore necessary to evaluate both performance and risk simultaneously, rather than treating geological modeling, reservoir simulation, and geomechanics as separate tasks. However, primary limitation of the workflow is data availability, particularly for deep HSA systems where thermal, petrophysical, and stress data are sparse. The approach therefore emphasizes uncertainty quantification rather than deterministic prediction, enabling evaluation of development scenarios across a range of plausible subsurface conditions..

A key outcome of this work is that uncertainty in permeability distribution, reservoir connectivity, and in-situ stress conditions often has a greater impact on project feasibility than uncertainty in temperature alone. The iterative workflow allows these uncertainties to be progressively reduced through targeted data acquisition and model updating. Although the workflow was developed for hot sedimentary aquifers, the methodology is broadly applicable to other geothermal settings where coupled thermo–hydro–mechanical processes control reservoir performance and operational risk. As such, the workflow provides a practical framework for geothermal screening, concept selection, and early-stage development planning under uncertainty.

REFERENCES

Baird, K.: A Novel Workflow for Geothermal Reservoir Characterisation: Understanding the Impact of Geological Heterogeneity on Geothermal Energy Production from Hot Sedimentary Aquifers, PhD Thesis, Heriot-Watt University, Edinburgh, UK (2025), unpublished.

Birdsell, D., Adams, B.M., and Saar, M.O.: Geothermal energy development in sedimentary basins: Opportunities and challenges, Geothermal Energy (2024).

Blackwell, D.D., and Richards, M.: *Geothermal Map of North America*, American Association of Petroleum Geologists, Tulsa, USA (2004).

Bullard, E.C.: Heat flow in South Africa, Proceedings of the Royal Society A, 173 (1939), 474–502.

Caers, J.: *Modeling Uncertainty in the Earth Sciences*, Wiley-Blackwell, Chichester, UK (2011).

Carslaw, H.S., and Jaeger, J.C.: Conduction of Heat in Solids, Oxford University Press, London, UK (1959).

Dvorkin, J., Nur, A., and Yin, H.: Effective properties of cemented granular materials, Mechanics of Materials (2009).

Ellsworth, W.L.: Injection-Induced Earthquakes, *Science*, 341 (2013), 1225942.
Barton, C.A., Zoback, M.D., and Moos, D.: Fluid Flow Along Potentially Active Faults in Crystalline Rock, *Geology*, 23 (1995), 683–686.

Finsterle, S.: Practical Approaches to Uncertainty Quantification in Subsurface Modeling, *Computers & Geosciences*, 85 (2015), 23–32.

Grant, M.A., Donaldson, I.G., and Bixley, P.F.: *Geothermal Reservoir Engineering*, 2nd ed., Academic Press, Oxford, UK (2011).

Haldorsen, H.H., and Lake, L.W.: A New Approach to Shale Management in Scale-Up of Reservoir Models, *Society of Petroleum Engineers Journal*, 24 (1984), 447–457.

Horner, D.R.: Pressure build-up in wells, Proceedings of the Third World Petroleum Congress, The Hague (1951).

Journel, A.G., and Huijbregts, C.J.: *Mining Geostatistics*, Academic Press, London, UK (1978).

Khalili, M., and Ahmadi, M.: Reservoir modeling simulation: Advancements, challenges and future perspectives, (2024).

Limberger, J., Boxem, T., Pluymaekers, M., Bruhn, D., Manzella, A., Calcagno, P., Beekman, F., Cloetingh, S., and van Wees, J.D.: Geothermal energy in deep aquifers: A global assessment of the resource base for direct heat utilization, Renewable and Sustainable Energy Reviews, 82 (2018), 961–975.

Majer, E.L., Baria, R., Stark, M., et al.: Induced Seismicity Associated with Enhanced Geothermal Systems, *Geothermics*, 36 (2007), 185–222.

Moeck, I.: Catalog of geothermal play types based on geologic controls, Renewable and Sustainable Energy Reviews, 37 (2014), 867–882.

Ringrose, P., and Bentley, M.: *Reservoir Model Design: A Practitioner's Guide*, Springer, Dordrecht, Netherlands (2015).

Rühaak, W., Cherubini, Y., and Sass, I.: Sensitivity of geothermal energy production to reservoir properties, Energy Procedia, 76 (2015), 64–71.

Rutqvist, J.: Fractured Rock Stress–Permeability Coupling and Application to Geothermal Systems, *Journal of Geophysical Research: Solid Earth*, 120 (2015), 252–273.

Wang, Y., Voskov, D., Khait, M., Saeid, S., and Bruhn, D.: Influential factors on the development of a low-enthalpy geothermal reservoir: A sensitivity study of a realistic field, Renewable Energy, 179 (2021), 641–651.

Zoback, M.D.: *Reservoir Geomechanics*, Cambridge University Press, Cambridge, UK (2010).

Zang, A., and Stephansson, O.: *Stress Field of the Earth's Crust*, Springer, Berlin, Germany (2010).